(1)

OFFICE OF NAVAL RESEARCH

Contract N00014-92-J-1183, Mod/Amend P00001

R&T Code 413d017

Technical Report No. 13

Fabrication and Characterization of Pt and Pt-Ir Ultramicroelectrodes

by

George J. Cali and Nathan S. Lewis,

California Institute of Technology
Department of Chemistry
Pasadena, California 91125

May 31, 1992

REPORT DOCUMENTATION PAGE

Form Approved
OMB No 0704-0188

1. AGENCY USE ONLY (Leave blank)	2. REPORT DATE	3. REPORT TYPE AND DATES COVERED
	May 31, 1992	End-of-Year, 1 June 91/31 May 92

4. TITLE AND SUBTITLE

Fabrication and Characterization of Pt and Pt-Ir Ultramicroelectrodes.

5. FUNDING NUMBERS

N00014-92-J-1183
Mod/Amend P00001

6. AUTHOR(S)

George J. Cali and Nathan S. Lewis

7. PERFORMING ORGANIZATION NAME(S) AND ADDRESS(ES)

California Institute of Technology 127-72
Division of Chemistry and Chemical Engineering
Pasadena, California 91125

8. PERFORMING ORGANIZATION REPORT NUMBER

9. SPONSORING/MONITORING AGENCY NAME(S) AND ADDRESS(ES)

Dr. Ronald A. De Marco
Chemistry Division
Office of Naval Research
800 North Quincy Street
Arlington, Virginia 22217-5000

10. SPONSORING/MONITORING AGENCY REPORT NUMBER

11. SUPPLEMENTARY NOTES

12a. DISTRIBUTION/AVAILABILITY STATEMENT

This document has been approved for public release and sale; its distribution is unlimited.

12b. DISTRIBUTION CODE

13. ABSTRACT (Maximum 200 words)

Freshly etched Pt and Pt-Ir ultramicroelectrode tips have hemispherical radii of respectively 0.36 ± 0.20 and 0.57 ± 0.24 um (95% confidence limits), as determined analytically from SEM micrographs. These values and variations in the subsequent glass-coating step necessary to insulate the tip from the ultramicroelectrode shaft effectively limit the size of the smallest ultramicroelectrodes that can be reliably prepared.

14. SUBJECT TERMS

Pt, Pt-Ir, Ultramicroelectrodes

15. NUMBER OF PAGES

13

16. PRICE CODE

17. SECURITY CLASSIFICATION OF REPORT	18. SECURITY CLASSIFICATION OF THIS PAGE	19. SECURITY CLASSIFICATION OF ABSTRACT	20. LIMITATION OF ABSTRACT

Recent work (1, 2) has detailed the preparation of conical and hemispherical Pt-Ir ultramicroelectrodes using a two-step procedure involving an electrochemical etch and the sealing of the resulting sharp wire tip by translation through molten glass. The ultramicroelectrodes were characterized by scanning electron microscopy (SEM) and electrochemically (1, 2). In this work, the same experimental procedure is extended to the fabrication of Pt ultramicroelectrodes. A new method is described for the characterization of the tip geometry, the electrochemical response of Pt ultramicroelectrodes to $Ru(NH_3)_6^{2+/3+}$ in water and to $FeCp_2^{0/+}$ and $Co(CpCOOCH_3)_2^{0/+}$ in acetonitrile is reported, and aspects related to ultramicroelectrode reliability are addressed.

SEM micrographs of freshly etched Pt and Pt-Ir wires are shown in Fig. 1, and the method for characterizing the tip geometry is outlined in Fig. 2. Based on this method, freshly etched Pt and Pt-Ir wires have hemispherical radii at their apex of respectively 0.36 ± 0.20 and 0.57 ± 0.24 μm (95% confidence limits). The wires appeared smooth under the highest magnification available by SEM (40,000x), indicating that the NaOH/KCN etch employed (1, 2) effectively electropolishes the electrode surface as it etches material away (3). The early stages of the necking mechanism leading to the formation of the sharp tip can be seen in Fig. 3. The values obtained by the method in Fig. 2 confirm earlier estimates (1, 2) and are similar to those obtained by alternate methods of Pt ultramicroelectrode fabrication relying on Wollaston wire (4, 5), the pulling of annealed Pt wire (6), or molten salt etches (7). The advantage of the procedure employed here is that it can lead to the formation of ultramicroelectrodes with hemispherical and conical tip geometries, which tends to simplify the description of mass transport processes to the electrode surface (2).

Table I shows the limiting currents, half-wave potentials, and apparent electrochemical radii obtained from steady-state voltammograms for the reduction

odes

Dist | Avail. and / or Special

A-1

of $Ru(NH_3)_6^{3+}$ at Pt ultramicroelectrodes of various sizes. The apparent electrode radii r_{app} were determined from the voltammetric limiting current i_l and the relation $r_{app} = i_l / 2\pi nFCD$ (8). The sigmoidal shape of the voltammograms and the resulting limiting currents remained unchanged at the two scan rates employed, 10 and 100 mV s^{-1}. Table II in turn shows the response of a significantly larger ultramicroelectrode to $FeCp_2^{0/+}$ and $Co(CpCOOCH_3)_2^{0/+}$ in acetonitrile (9). In this case noticeable cathodic and anodic current peaks resulting from mass-transport limitations to the electrode surface appeared as the scan rate was increased (2). These waves reflect contributions from linear diffusion processes arising from the exposed conical portion of the electrode tip (see Fig. 1).

Tables I and II show that it is possible to fabricate Pt ultramicroelectrodes by the two-step etch-coat method employed (1, 2) with apparent electrochemical radii in the range from 20 to less than 0.1 μm. The measurement of apparent radii smaller than what can be expected from the freshly etched radii reported above has to be interpreted with caution. Extremely small limiting currents could be an artifact of the method of ultramicroelectrode fabrication resulting from cracks or fissures on an otherwise insulating glass sheath enveloping the ultramicroelectrode tip (10-12). Ultramicroelectrodes of this type act as Site Exclusion Electrochemical Detectors (SEEDS) and may well find important uses in the study of chemical and mass-transport properties in confined spaces; restricted mass transport may have important ramifications in the understanding of corrosion rates through cracks or fissures in metals resulting from metal fatigue, stress fractures, or defective welds, and in the accurate determination of the efficiencies of batteries and flow-through catalytic systems. Applications as microsampling sensing devices can also be envisioned. An alternative explanation for the measurement of electrochemical radii of less than 0.1 μm is that the translation of the freshly etched ultramicroelectrode tip through hot molten glass during the second step of the two-

step fabrication procedure (1, 2) causes the smooth electropolished surface seen in Fig. 1 to roughen considerably, leading to the exposure of extremely small surfaces of bare metal through textured glass. The effect has been observed by SEM (2). The resulting nanometer-sized electrodes (nanodes) would be considerably smaller than can be fabricated by alternate methods (4-7), and so would constitute a milestone in the fabrication of ultramicroelectrodes because they would be small enough to address fundamental questions in interfacial electrochemistry, for example the measurement of contributions due to solvent relaxation effects to reorganization energies (13) and the determination of heterogeneous electron transfer rate constants, as was recently attempted (14).

It would be desirable to differentiate conclusively between SEEDS and nanodes by experimental means. The smallest ultramicroelectrodes in this work were found to be unstable upon drying overnight, as reflected in dramatically increased voltammetric currents. This limits the use of SEM and TEM, which require evacuation. The establishment of a tunneling current by STM could be used in principle to establish that nanometer-sized patches of metal are indeed exposed, but this approach relies on the exposed metal, as opposed to surrounding glass, being oriented closest to the surface being used as a probe, which is however not a necessary condition for the functioning of nanodes. Transient current measurements in the microsecond time domain have been suggested (11), but an accurate interpretation of the results would depend on the ultramicroelectrode geometry assumed in the calculation, which is not known. Finally, the simultaneous measurement of half-wave potentials for two redox couples with different electron transfer rate constants could also be used to differentiate between SEEDS and nanodes (15, 16). A measured shift in the half-wave potential of the slower couple relative to the faster one should continue to increase as the ultramicroelectrode radius is decreased beyond 0.1 μm.

REFERENCES

1. M. J. Heben, M. M. Dovek, N. S. Lewis, R. M. Penner, and C. Q. Quate, *J. Microsc.* **152**, 651 (1988).

2. R. M. Penner, M. J. Heben, and N. S. Lewis, *Anal. Chem.* **61**, 1630 (1989).

3. G. Petzow, Metallographic Etching; American Society for Metals; Metals Park, OH, 1978.

4. A. M. Bond, M. Fleischmann, and J. Robinson, *J. Electroanal. Chem.* **168**, 299 (1984).

5. C. D. Baer, N. J. Stone, D. A. Sweigart, *Anal. Chem.* **60**, 188 (1988).

6. B. D. Pendley and H. D. Abruna, Anal. Chem. **62**, 782 (1990).

7. K. Itaya, T. Abe, and I. Uchida, *J. Electrochem. Soc.* **134**, 1191 (1987).

8. Z. Galus, Fundamentals of Electrochemical Analysis; Halstead Press, New York, 1976; Chapter 4.

9. J. B. Cooper and A. M. Bond, *J. Electroanal. Chem.* **315**, 143 (1991).

10. A. S. Baranski, *J. Electroanal. Chem.* **307**, 287 (1991).

11. K. B. Oldham, *Anal. Chem.* **64**, 646 (1992).

12. K. B. Oldham, *J. Electroanal. Chem.* **323**, 53 (1992).

13. R. A. Marcus, *J. Phys. Chem.* **95**, 2010 (1991).

14. R. M. Penner, M. J. Heben, T. L. Longin, and N. S. Lewis, *Science* **250**, 1118 (1990).

15. K. B. Oldham and C. G. Zoski, *J. Electroanal. Chem.* **256**, 11 (1988).

16. K. B. Oldham, C. G. Zoski, A. M. Bond, and D. A. Sweigart, *J. Electroanal. Chem.* **248**, 467 (1988).

Table I. Limiting currents, half-wave potentials, and apparent electrochemical radii obtained from steady-state voltammograms for the reduction of 2.8 mM $Ru(NH_3)_6Cl_3$ in 500 mM KCl. $r_{app} = i_l/2\pi nFDC$ (8).

Scan rate/mV s^{-1}	$E_{1/2}$/mV	i_l/nA	$r_{app}/\mu m$
10	-208	14	9.6
100	-208	13	9.5
10	-208	6.1	4.4
100	-205	6.0	4.3
10	-209	3.6	2.6
100	-209	3.7	2.6
10	-209	0.34	0.24
100	-210	0.33	0.23
10	-208	0.093	0.066
100	-210	0.090	0.064

Table II. Limiting currents, half-wave potentials, and apparent electrochemical radii obtained from steady-state voltammograms for the reduction of 0.48 mM $Co(CpCOOCH_3)_2PF_6$ and the oxidation of 0.50 mM $FeCp_2$ in 50 mM Bu_4NClO_4 in acetonitrile. $r_{app} = i_l/2\pi nFDC$ (8).

	$Co(CpCOOCH_3)_2$			$FeCp_2$		
rate/mV s^{-1}	$E_{1/2}$/mV	i_l/nA	r_{app}/μm	$E_{1/2}$/mV	i_l/nA	r_{app}/μm
5	-405	5.6	17	396	13	17
10	-404	5.5	17	395	12	17
20	-403	5.7	17	394	12	17
50	-399	6.1	19	392	13	18
100	-398	6.8	21	390	14	19
500	-398	8.1	25	391	16	22

FIGURE CAPTIONS

Figure 1. SEM micrographs (10,000x magnification) of freshly etched (1, 2) Pt (r = 0.27 μm, left) and Pt-Ir (r = 0.47 μm, right). The radii were determined as outlined in Fig. 2. Freshly etched Pt and Pt-Ir wires (1, 2) have hemispherical radii at their apex of respectively 0.36 ± 0.20 and 0.57 ± 0.24 μm (95% confidence limits). These values confirm earlier estimates (1, 2).

Figure 2. Diagram illustrating the method used for the determination of the apex radii of freshly etched (1, 2) Pt and Pt-Ir. The radii were obtained by equating the curvature of the parabola at its apex, $K_p = 2a/(1 + b^2)^{3/2}$, to the curvature of the inscribed circle $K_c = 1/r$. The parameters a, b and c were determined analytically from micrographs like those of Fig. 1 and measurements at the positions represented by the dots.

Figure 3. (Left) SEM micrograph of freshly etched 0.020" wire emersed immediately before the breakoff transition described in Fig. 1 of reference (1). (Right) Similar experiment, immediately after breakoff. Note that these micrographs were obtained at a much lower magnification than those of Fig. 1.

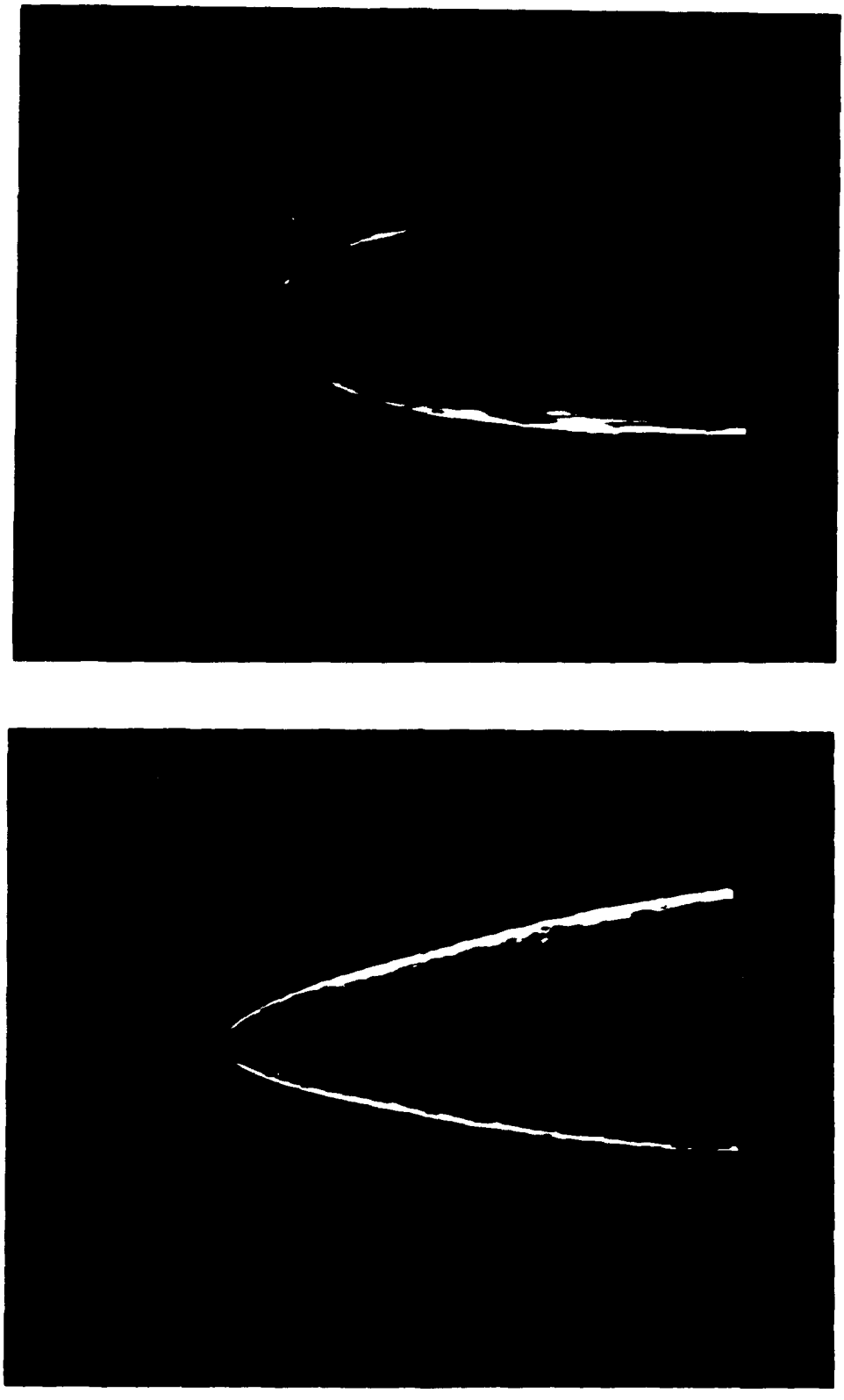

Figure 1
Fabrication and Characterization ...

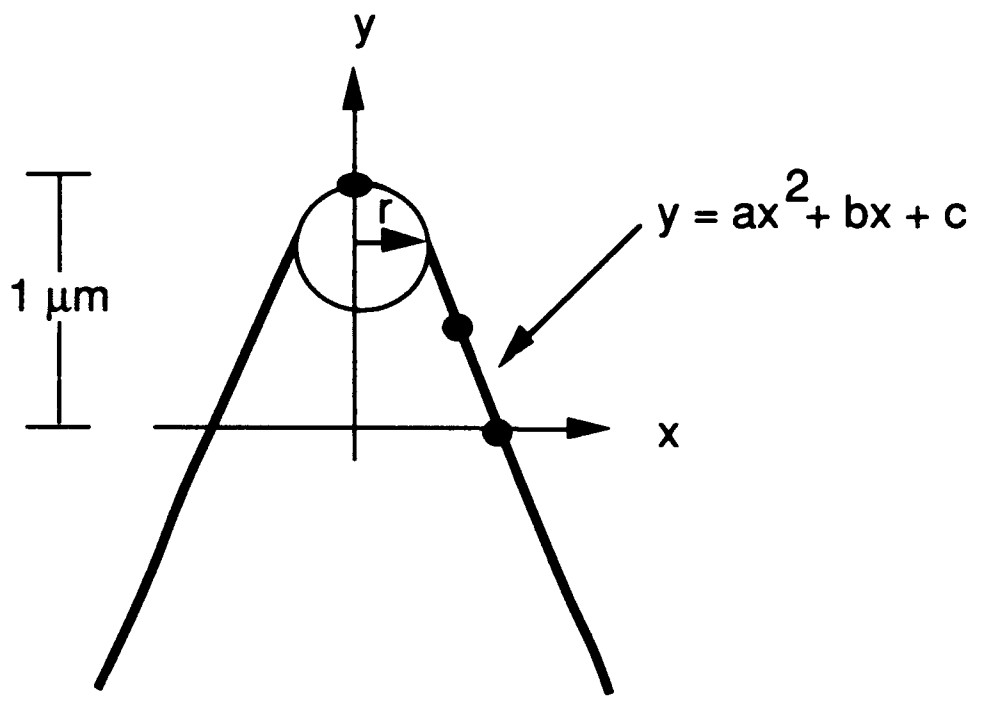

Figure 2
Fabrication and Characterization ...

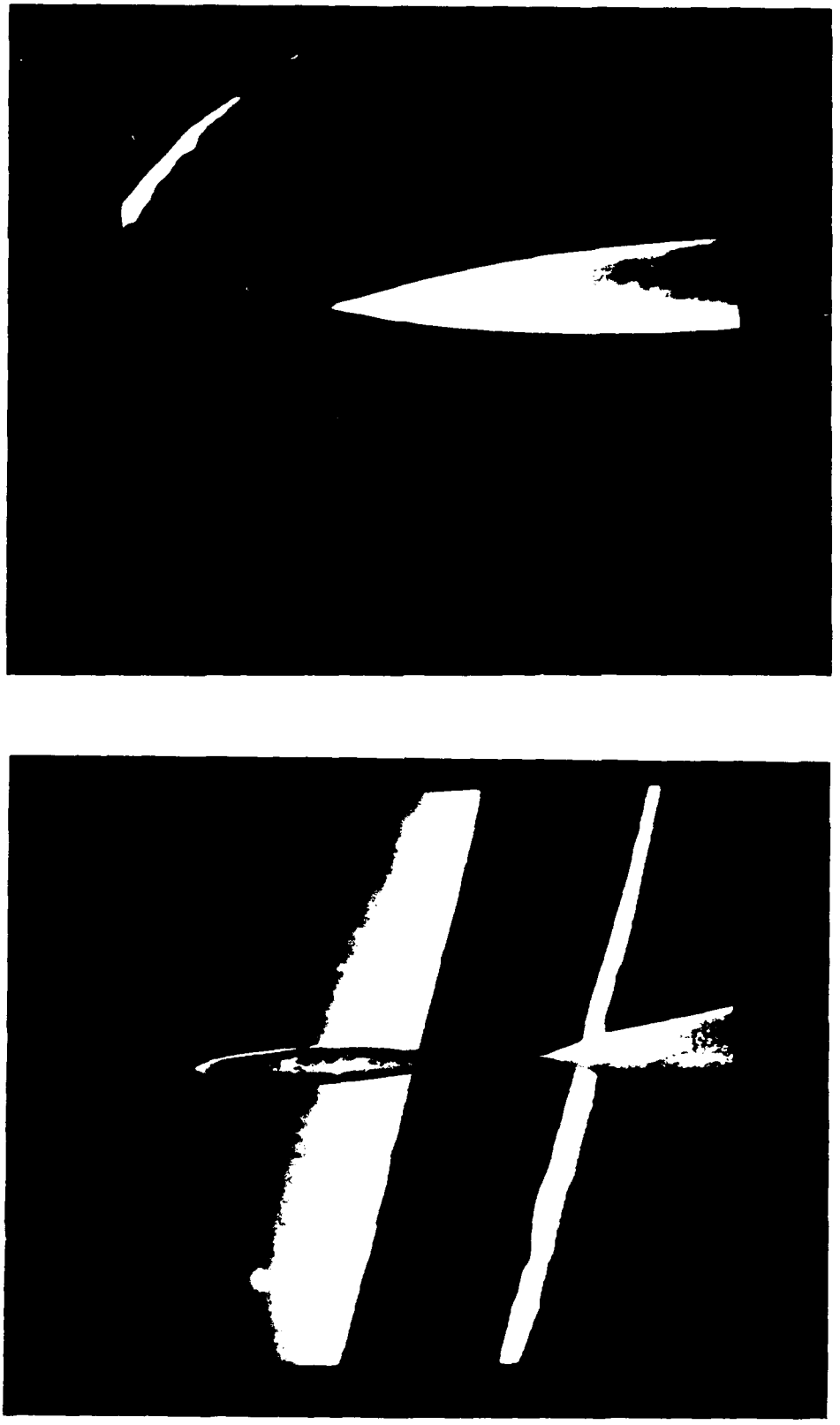

Figure 3
Fabrication and Characterization ...

TECHNICAL REPORT DISTRIBUTION LIST - GENERAL

Office of Naval Research (2)*
Chemistry Division, Code 1113
800 North Quincy Street
Arlington, Virginia 22217-5000

Dr. James S. Murday (1)
Chemistry Division, Code 6100
Naval Research Laboratory
Washington, D.C. 20375-5000

Dr. Robert Green, Director (1)
Chemistry Division, Code 385
Naval Air Weapons Center
Weapons Division
China Lake, CA 93555-6001

Dr. Elek Lindner (1)
Naval Command, Control and Ocean
Surveillance Center
RDT&E Division
San Diego, CA 92152-5000

Dr. Bernard E. Douda (1)
Crane Division
Naval Surface Warfare Center
Crane, Indiana 47522-5000

Dr. Richard W. Drisko (1)
Naval Civil Engineering
Laboratory
Code L52
Port Hueneme, CA 93043

Dr. Harold H. Singerman (1)
Naval Surface Warfare Center
Carderock Division Detachment
Annapolis, MD 21402-1198

Dr. Eugene C. Fischer (1)
Code 2840
Naval Surface Warfare Center
Carderock Division Detachment
Annapolis, MD 21402-1198

Defense Technical Information
Center (2)
Building 5, Cameron Station
Alexandria, VA 22314

* Number of copies to forward